Available on CMS information server

CMS CR -2016/078

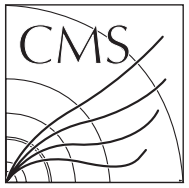

The Compact Muon Solenoid Experiment

Conference Report

Mailing address: CMS CERN, CH-1211 GENEVA 23, Switzerland

07 May 2016 (v3, 13 May 2016)

Results and Prospects for $\mathrm{t\bar{t}H}$ at CMS

Johannes Hauk for the CMS Collaboration

Abstract

First results of associated top-quark pair and Higgs-boson production ($\mathrm{t\bar{t}H}$) at CMS from the LHC Run 2 era at centre-of-mass energy $\sqrt{s} = 13\,\mathrm{TeV}$ are presented. The $\mathrm{t\bar{t}H}$ process is the only one allowing a direct measurement of the top-Higgs coupling, which is an important test of the Standard Model (SM), and for searching new physics. Three analyses are performed and optimised individually according to different Higgs boson decays, and results are obtained in each for the signal strength $\mu = \sigma/\sigma_{\mathrm{SM}}$ being the cross-section ratio of the measurement to the SM prediction. The diphoton decay $\mathrm{t\bar{t}H}(\gamma\gamma)$ results in $\mu = 3.8^{+4.5}_{-3.6}$, the decays with leptons in the final state $\mathrm{t\bar{t}H}$(multileptons) in $\mu = 0.6^{+1.4}_{-1.1}$, and the decay to a bottom quark pair $\mathrm{t\bar{t}H}(\mathrm{b\bar{b}})$ yields $\mu = -2.0 \pm 1.8$. A combined result of $\mu_{\mathrm{t\bar{t}H}} = 0.15^{+0.95}_{-0.81}$ is obtained from a fit to all three channels. No significant deviation from the SM is observed.

Presented at *Moriond/EW2016 51st Rencontres de Moriond on Electroweak Interactions and Unified Theories*

Results and Prospects for $t\bar{t}H$ at CMS

Johannes Hauk for the CMS Collaboration
Deutsches Elektronen-Synchrotron DESY, Notkestrasse 85, 22607 Hamburg, Germany

First results of associated top-quark pair and Higgs-boson production ($t\bar{t}H$) at CMS from the LHC Run 2 era at centre-of-mass energy $\sqrt{s} = 13\,\text{TeV}$ are presented. The $t\bar{t}H$ process is the only one allowing a direct measurement of the top-Higgs coupling, which is an important test of the Standard Model (SM), and for searching new physics. Three analyses are performed and optimised individually according to different Higgs boson decays, and results are obtained in each for the signal strength $\mu = \sigma/\sigma_{\text{SM}}$ being the cross-section ratio of the measurement to the SM prediction. The diphoton decay $t\bar{t}H(\gamma\gamma)$ results in $\mu = 3.8^{+4.5}_{-3.6}$, the decays with leptons in the final state $t\bar{t}H(\text{multileptons})$ in $\mu = 0.6^{+1.4}_{-1.1}$, and the decay to a bottom quark pair $t\bar{t}H(b\bar{b})$ yields $\mu = -2.0 \pm 1.8$. A combined result of $\mu_{t\bar{t}H} = 0.15^{+0.95}_{-0.81}$ is obtained from a fit to all three channels. No significant deviation from the SM is observed.

1 Introduction and Process Overview

One of the highlights of the Run 1 period at LHC was the discovery of a Higgs boson with mass $m_{\text{H}} \approx 125\,\text{GeV}$ by the ATLAS and CMS experiments in 2012 [1,2], using proton-proton collisions at centre-of-mass energies of $\sqrt{s} = 7\,\text{TeV}$ and $8\,\text{TeV}$. After the discovery the focus lies on measuring the properties of the new particle to answer the two central questions. Is it the Higgs boson as predicted by the Standard Model of Particle Physics (SM), and irrespective of this, does it reveal signs of new physics beyond the SM? One central aspect to answer these questions is to measure the coupling constants of the boson to the other elementary particles, which depend according to the SM on the mass. The top quark as the heaviest elementary particle has the strongest coupling of all. A direct measurement of the top-Higgs Yukawa coupling is amongst the priorities of the Run 2 era of LHC, which started in 2015 with an increased energy $\sqrt{s} = 13\,\text{TeV}$ – first results towards this measurement are shown in this report.

Some Feynman diagrams for different Higgs boson production mechanisms are shown in Figure 1. At the LHC, the main process is gluon-gluon fusion, where quark loops are involved, as the Higgs boson does not couple directly to massless gluons; especially the top quark contributes here, but also the lighter quarks, and potentially unknown particles. Processes with couplings to the electroweak $W^{\pm}$ and Z^0 gauge bosons ('W' and 'Z' in the following) contribute with significantly smaller cross sections, the vector boson fusion and the Higgs strahlung. The associated top-quark pair ($t\bar{t}$) and Higgs boson production, $t\bar{t}H$, is a factor of about 200 (100) smaller than the inclusive cross section at 8 TeV (13 TeV). In principle also the associated production with a single top quark is possible, but is suppressed in the SM by interference from couplings of the Higgs boson to the top quark and the W – in certain theories beyond the SM this contribution is enhanced and needs to be considered also in corresponding $t\bar{t}H$ interpretations, but the present study focuses on SM compatibility. The top-Higgs coupling thus occurs in the measurable processes gluon-gluon fusion and $t\bar{t}H$. In the former however, as loop contributions from other quarks are and from unknown particles could be present, a direct coupling measurement is not

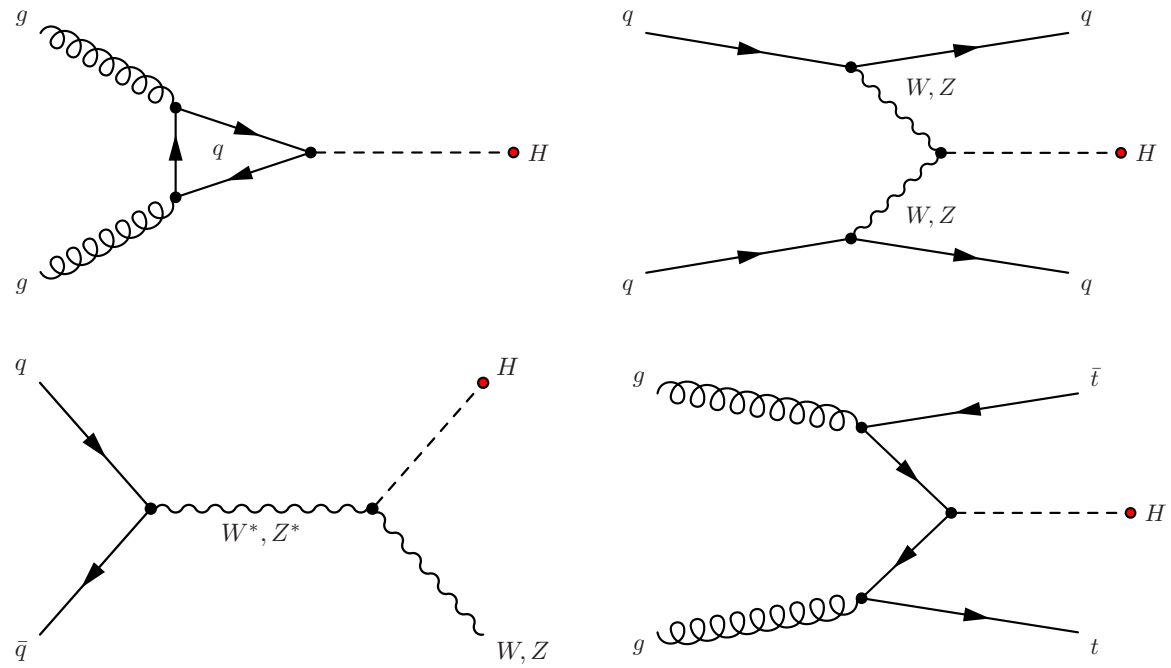

Figure 1 – Leading order Feynman diagrams of Higgs boson production at LHC: gluon-gluon fusion (top left), vector boson fusion (top right), Higgs strahlung (bottom left) and top-pair associated production (bottom right).

possible; only indirect constraints using a certain model for interpretation can be deduced. The only possibility to measure the top-Higgs coupling is $t\bar{t}H$. Once the coupling is obtained, it can be in turn used to search for hidden loop contributions in gluon-gluon fusion. This report presents the first $t\bar{t}H$ results from CMS at $\sqrt{s} = 13\,\text{TeV}$ using the 2015 dataset. The $t\bar{t}H$ cross section increases by a factor 3.8 when going from 8 TeV to 13 TeV. The integrated luminosity of the analyzed dataset corresponds to 2.3-2.7 fb^{-1}, which is equivalent to about 50% of the accumulated 8 TeV data sample. The dominant background processes for each $t\bar{t}H$ analysis channel are $t\bar{t}$ in association with other particles, which have a similar cross section increase.

The $t\bar{t}H$ decays lead to very complex final states. As the top quark decays almost always to a bottom quark and a W, the decays of the $t\bar{t}$ system are categorized by the decays of the two W bosons: 'dileptons' for two leptonic W decays which has the smallest branching ratio but leads to cleanest signatures, 'l+jets' for a leptonic and a hadronic decay, and 'hadronic' for two hadronic decays. The Higgs boson cannot decay into top quarks, they are too heavy; the decay does not explicitly provide access to the top-Higgs coupling. The three relevant processes which can be experimentally identified are categorized as follows. The dominant decay $H(b\bar{b})$ is into bottom quarks, being the heaviest particles which can be produced real, with about 57% probability. Leptonic final states H(multileptons) arise not from leptonic decays of the Higgs boson itself, but from decays to WW* or ZZ* (one of them being virtual) or τ leptons, and subsequent leptonic decay of at least one of them. The decay into photons $H(\gamma\gamma)$ has a small branching ratio of about 0.2% but a very clean signature; also here loops are involved in the coupling to massless photons, where besides the top quark the W contributes and potentially unknown particles. The $t\bar{t}H$ analyses are separated by Higgs boson decay into $t\bar{t}H(b\bar{b})$, $t\bar{t}H$(multileptons) and $t\bar{t}H(\gamma\gamma)$, both for the Run 1 analysis and the results presented here – each uses an own analysis strategy, and is further subdivided according to the $t\bar{t}$ decay.

A summary of the Run 1 signal strength μ measurements is given in [3], where $\mu = \sigma/\sigma_{\text{SM}}$ is defined as the ratio of the measured production rate to the SM prediction. The main analysis strategy was to measure the rates of different Higgs production and decay mechanisms and to combine the results, identifying the channel via the different final state topologies. In general a good agreement with the SM expectation is found. The signal strength for the different Higgs production mechanisms and the combined strength are matching the predictions, except

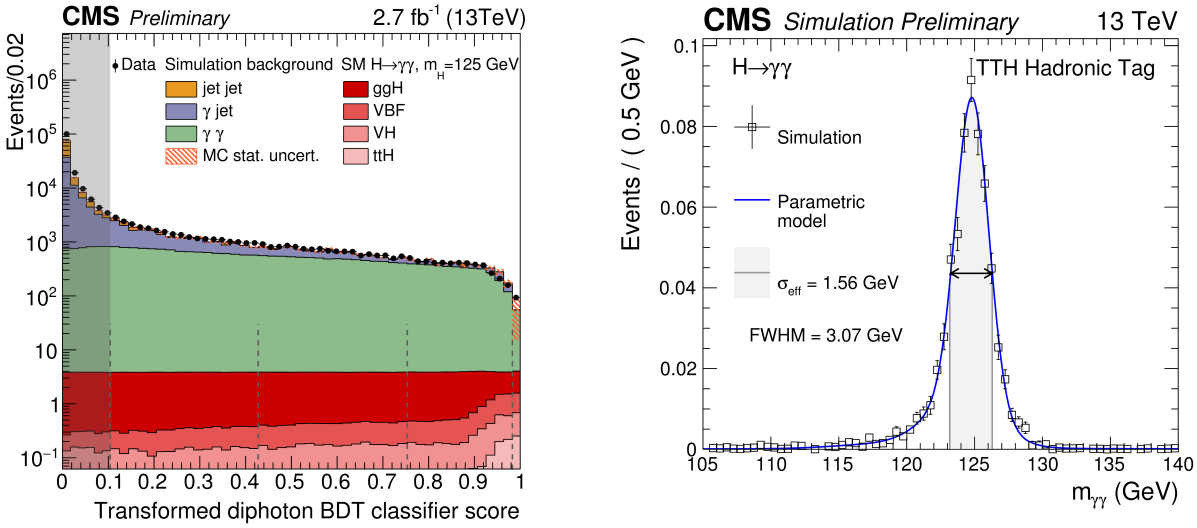

Figure 2 – Left: diphoton BDT classifier distribution. The vertical dashed lines indicate different categories for gluon-gluon fusion, the thresholds for $t\bar{t}H$ are stated in the text. Right: effective diphoton mass resolution in the hadronic channel, obtained from a parametric model fit to the simulated signal.

of the $t\bar{t}H$ process which is slightly above, mainly due to an excess of events in the CMS $t\bar{t}H$(multileptons) analysis. The result of $\mu_{t\bar{t}H} = 2.3^{+0.7}_{-0.6}$ corresponds to an observed (expected) significance of 4.4σ (2.0σ) over the null hypothesis. The results are obtained from a combined fit of all analysis channels, but the $t\bar{t}H$ results are dominated by the direct measurements in the three channels $t\bar{t}H(b\bar{b})$, $t\bar{t}H$(multileptons) and $t\bar{t}H(\gamma\gamma)$.

2 Analysis Strategy and Results

For each of the channels $t\bar{t}H(b\bar{b})$, $t\bar{t}H$(multileptons) and $t\bar{t}H(\gamma\gamma)$ an independent analysis is performed. In each, the corresponding dominant reducible and irreducible background processes are $t\bar{t}$ associated with other particles. As their cross sections are above the signal one, a good understanding of them and good signal-to-background separation is important. Each analysis classifies events into two decay channels based on the lepton multiplicity, and results are obtained from a simultaneous fit of these – in $t\bar{t}H(\gamma\gamma)$ and $t\bar{t}H(b\bar{b})$ these represent the $t\bar{t}$ decays, while in $t\bar{t}H$(multileptons) leptons also occur from the Higgs boson decay chain. The analyses are optimised according to the rather low statistics, and several analysis methods are improved compared to the Run 1 strategy. The results are interpreted in the SM using the signal strength.

2.1 $t\bar{t}H(\gamma\gamma)$

The $t\bar{t}H(\gamma\gamma)$ process has a small branching ratio, but a resonant diphoton mass as signature which can be well reconstructed due to the excellent photon identification and energy resolution. The main backgrounds stem from the irreducible $t\bar{t}+\gamma\gamma$ and the reducible $t\bar{t}$+jets producing fake photons. As loops contribute in the decay unknown physics could influence the results.

The analysis is an integral part of the inclusive $H(\gamma\gamma)$ analysis[4], where events are categorized according to production mode. It is performed on $2.7\,\text{fb}^{-1}$ of data preselected with diphoton triggers. Photon and diphoton reconstruction are identical to the inclusive analysis. The $t\bar{t}H$ contribution is enhanced by requiring signatures of the $t\bar{t}$ system, and is separated into the 'leptonic' (dileptons and l+jets) and 'hadronic' channels. At least 1 (exactly 0) leptons and at least 2 (at least 5) jets are required in the leptonic (hadronic) channel with at least 1 b-tag.

The main challenges are the suppression of fake photons and corresponding backgrounds, and to obtain an excellent diphoton mass resolution. This requires a good photon reconstruction

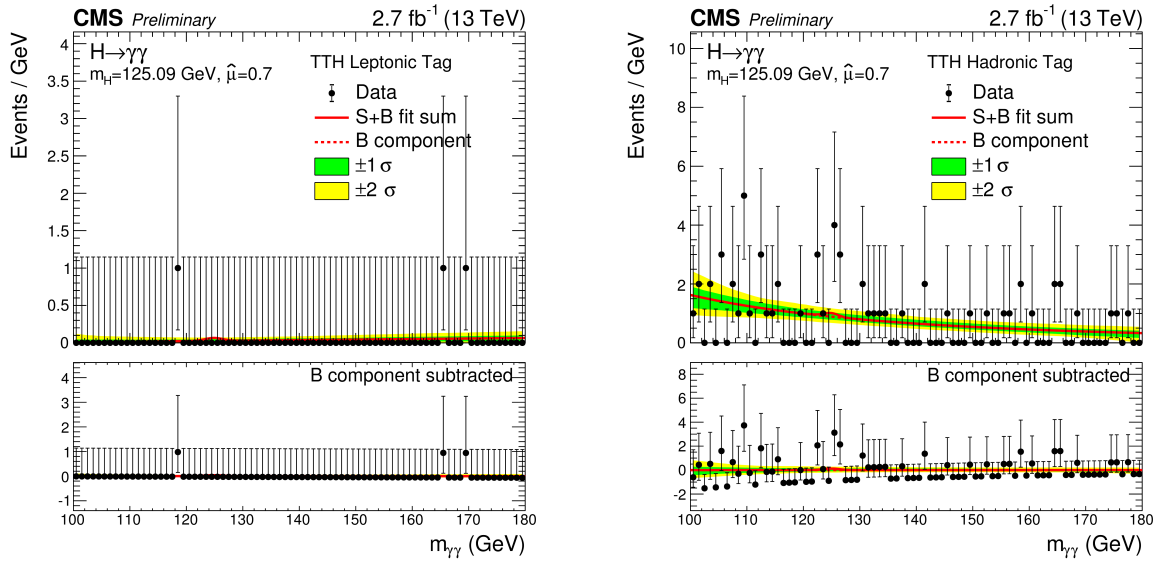

Figure 3 – Diphoton mass distribution and simultaneous fit of signal and background in the leptonic (left) and hadronic (right) channel, for the Run 1 best fit mass $m_{\mathrm{H}} = 125.09\,\mathrm{GeV}$ and the signal strength of the combined fit of the inclusive analysis of 0.7.

and energy calibration, but also the association to the correct primary vertex in the pileup environment. Different information is combined via a boosted desicion tree (BDT) which is used for photon identification. It is then subsequently used to classify diphoton events via another BDT for signal-like kinematic characteristics, events with good diphoton mass resolution and photon-like values from the photon identification BDT, while avoiding any dependence on the mass itself. This diphoton BDT classifier is used to further select events, requiring values above 0.246 (0.088) in the leptonic (hadronic) channel; the distribution is shown in Figure 2, together with the resulting effective diphoton mass resolution.

The event interpretation including signal and background models is identical the the inclusive analysis, searching for a diphoton mass resonance assuming a non-resonant background as seen in Figure 3. The signal is given as a parametric model including systematic variations as the sum of up to four Gaussians, obtained from simulation for different masses. Shape and normalisation for any mass point are obtained by continuous interpolation. For the background, smooth fit functions taking several functional forms are used, where a large set of function families is considered and treated as discrete parameter in a likelihood fit. The fit model is validated in control regions obtained by inverting the photon identification and loosening the event selection.

In the hadronic channel with higher statistics a small excess of events appears around m_{H}, while in the cleaner leptonic channel no events are observed in this region, but only three events are selected there in total. The combined observed signal strength of $\mu = 3.8^{+4.5}_{-3.6}$, estimated at the Run 1 best fit mass $m_{\mathrm{H}} = 125.09\,\mathrm{GeV}$, is within the large uncertainties compatible with the SM. The $\mathrm{t\bar{t}H}(\gamma\gamma)$ process allows a high-purity $\mathrm{t\bar{t}H}$ selection, resulting in a small impact of systematic uncertainties; the measurement is statistically limited.

2.2 $t\bar{t}H$ (multileptons)

The $\mathrm{t\bar{t}H}$(multileptons) analysis [5] targets at selecting events where the Higgs boson decays to $\tau^+\tau^-$, WW* or ZZ* with subsequent leptonic decay of at least one of the products, in combination with the dileptons or l+jets channels of $\mathrm{t\bar{t}}$, i.e. at least two leptons are present. It has the smallest irreducible backgrounds from $\mathrm{t\bar{t}}$ associated with vector bosons, $\mathrm{t\bar{t}W}$ and $\mathrm{t\bar{t}Z}$. Thus the focus lies on understanding the complex reducible background $\mathrm{t\bar{t}}$+jets with fake leptons.

The leptons are used for triggering, the analyzed dataset corresponds to $2.3\,\mathrm{fb}^{-1}$. Events are categorized into the 'dilepton' channel requiring exactly 2 leptons of same charge, and the

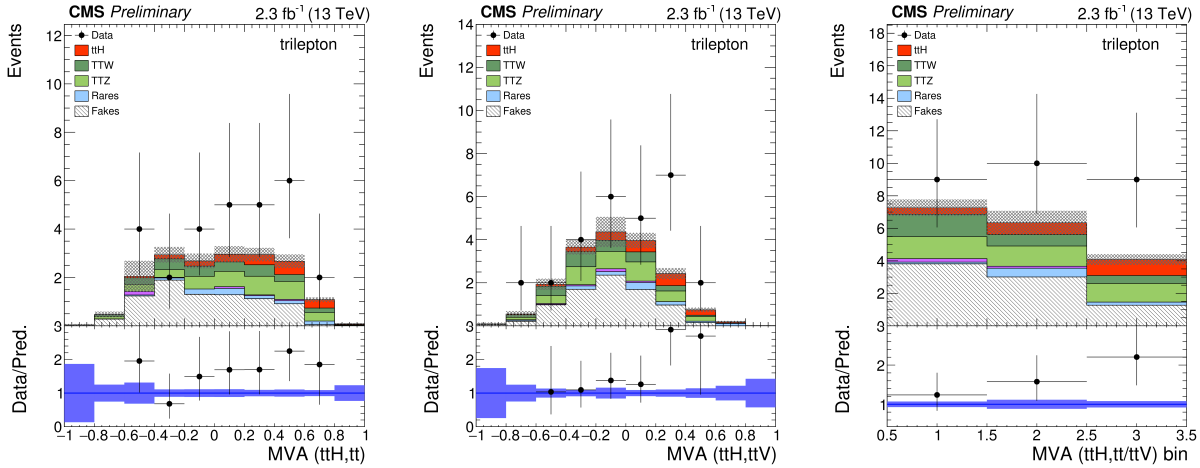

Figure 4 – Distribution of the BDT against the reducible (left) and irreducible (middle) background, and final discriminant from their two-dimensional space (right), in the trilepton channel.

'trilepton' channel requiring at least 3 leptons. The $t\bar{t}$ signature is enhanced by requiring at least 4 (at least 2) jets in the dilepton (trilepton) channel with at least 1 b-tag. The analysis strategy is optimised according to these channels, but to enhance the sensitivity events are further sub-categorized for the final combined fit according to different background compositions based on lepton flavour, lepton charge, presence of a hadronic τ decay, and presence of at least 2 b-tags.

The irreducible backgrounds are taken from simulation. Separation of prompt leptons from fake leptons, i.e. leptons from hadron decays in jets or mis-identified other particles, is obtained via a BDT. The modelling of the fake lepton backgrounds is acquired from control regions relaxing the lepton selection, and a transfer factor is applied. The fake rate is estimated from QCD multijet and Z+l events. For electrons also charge mis-reconstruction needs to be considered, and is estimated from the dilepton mass spectrum in events selected with same and with opposite charge electrons.

To separate signal from background, in each of the two channels two independent BDTs are constructed, one to separate against the reducible and one against the irreducible background. The final discriminant is then formed by dividing the two-dimensional space of the two classifiers into regions of different signal-to-background ratio. This discriminant is then fitted simultaneously in all sub-categories. The distributions of the BDT classifiers and the final discriminant are displayed in Figure 4.

In the trilepton channel an excess of events is observed with $\mu = 5.8^{+3.3}_{-2.7}$, however the dominant dilepton channel is below the expectation and yields $\mu = -0.5^{+1.0}_{-0.7}$. The combined result of $\mu = 0.6^{+1.4}_{-1.1}$ is in agreement with the SM. Splitting the dilepton channel via flavour shows also the mean value of the dimuon channel below the SM expectation.

2.3 $t\bar{t}H\,(b\bar{b})$

The $t\bar{t}H(b\bar{b})$ analysis [6] has the advantage of the highest Higgs boson branching ratio, and also the direct coupling to the final state particles is unambiguous and in first order independent of model assumptions. However, the background from tt+jets is overwhelming, and especially the association with two real b jets $t\bar{t}+b\bar{b}$ is irreducible and also theoretically challenging, thus not yet well understood. Another challenge comes from the presence of many jets with similar kinematics, making their association to $t\bar{t}$ or the Higgs boson ambiguous. As also the dijet mass resolution is by far worse than for the diphoton decays, no outstanding quantity for signal separation exists. The main strategy is to constrain the backgrounds forming many orthogonal categories of different signal and background composition, and to obtain a good signal separation.

The additional jets in $t\bar{t}$+jets, i.e. the jets not stemming from the $t\bar{t}$ decay but from additional

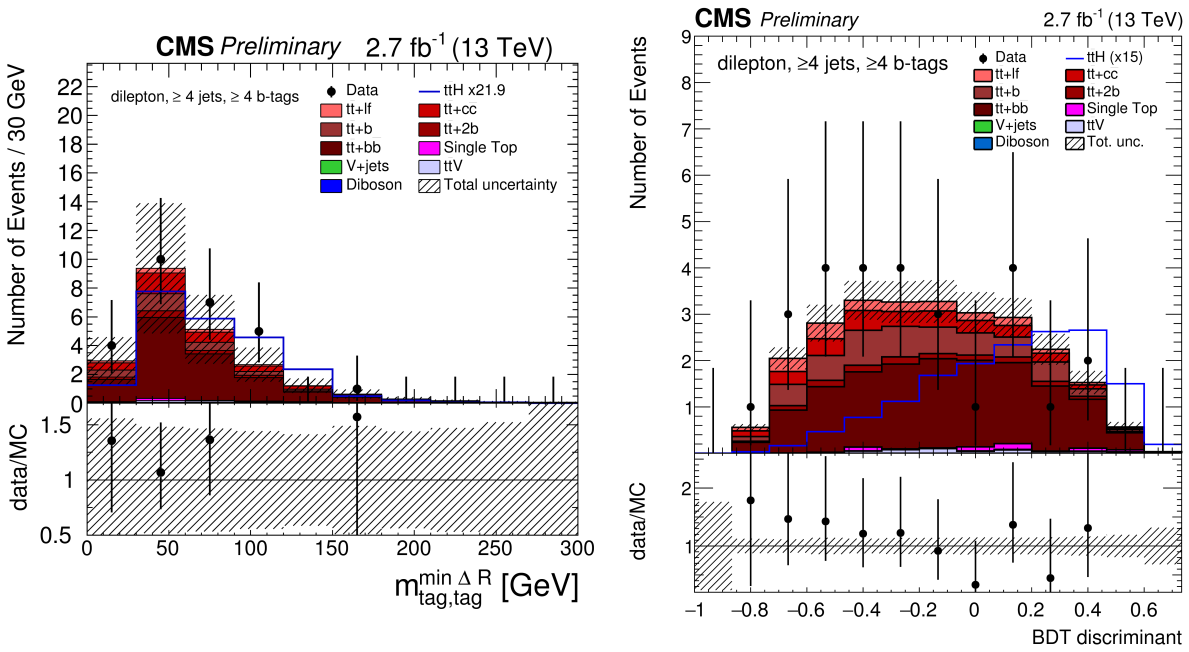

Figure 5 – Pre-fit expectation of the invariant mass of the b-tagged jet pair with minimal spatial separation in ΔR, which is one of the BDT input variables (left), and post-fit distribution of the final BDT discriminant (right), both shown for the dilepton category with at least 4 jets and b-tags. In the left plot the signal is normalised to the total background for shape comparisons, in the right a constant normalisation factor of 15 is used for visibility.

radiations, need to be split according to their heavy flavour content and treated as mainly independent contributions, as their modelling in simulation is not optimal as known from Run 1 analyses. The simulated $\mathrm{t\bar{t}}$+jets sample is segmented based on the method used in [7], using the jet clustering to define the jet flavour by injecting hadrons containing b or c quarks with momenta scaled to negligible values into the list of stable particles. The process $\mathrm{t\bar{t}+b\bar{b}}$ comprises two or more additional b jets, i.e. jets containing b hadrons. The presence of one additional b jet containing exactly one b hadron is labelled as $\mathrm{t\bar{t}}$+b. These two processes are in principle the same, in the latter case one of the jets is outside the detector acceptance; they could be treated perturbatively, but the massive quarks complicate this. The $\mathrm{t\bar{t}}$+2b process has one additional b jet which contains at least two b hadrons; this mainly occurs from collinear gluon splitting, and is theoretically and experimentally different from the previous. In simulation it comes mainly from the parton shower, and needs an arbitrary cut-off to avoid divergence, which is matter of tuning. In the presence of additional c jets similar issues appear, but since it is a less relevant background it is treated as a single process $\mathrm{t\bar{t}+c\bar{c}}$ which is inclusive for all events with at least one additional c jet. Other events are named $\mathrm{t\bar{t}}$+lf, as only light flavour jets occur.

The analysis is separated according to the lepton multiplicity of $\mathrm{t\bar{t}}$ into the 'dilepton' and the 'l+jets' channel. The leptons suppress the QCD multijet background and are used for triggering. To enhance the $\mathrm{t\bar{t}}$ topology, exactly 2 opposite-charge leptons are (exactly 1 lepton is) required in the dilepton (l+jets) channel, and the presence of at least 3 (at least 4) jets is required with at least 2 b-tags. The dilepton channel profits from minimal non-$\mathrm{t\bar{t}}$ backgrounds and minimal jet combinatorics, while the l+jets channel has high statistics due to the larger branching ratio.

In each of the two analysis channels, events are categorized according to their reconstructed jet and b-tag multiplicities. Background-like categories with low jet and especially b-tag multiplicity constrain the different backgrounds. Signal-like categories following the topology of $\mathrm{t\bar{t}H(b\bar{b})}$ have the highest signal-over-background ratios, and $\mathrm{t\bar{t}+b\bar{b}}$ is the dominant background. Five categories based on (jet, b-tag)-multiplicity are considered in the dilepton channel: (=3, =2), (≥4, =2), (=3, =3), (≥4, =3), (≥4, ≥4). Seven such categories are used in the l+jets channel: (≥6, =2), (=4, =3), (=5, =3), (≥6, =3), (=4, =4), (=5, ≥4), (≥6, ≥4). In addition,

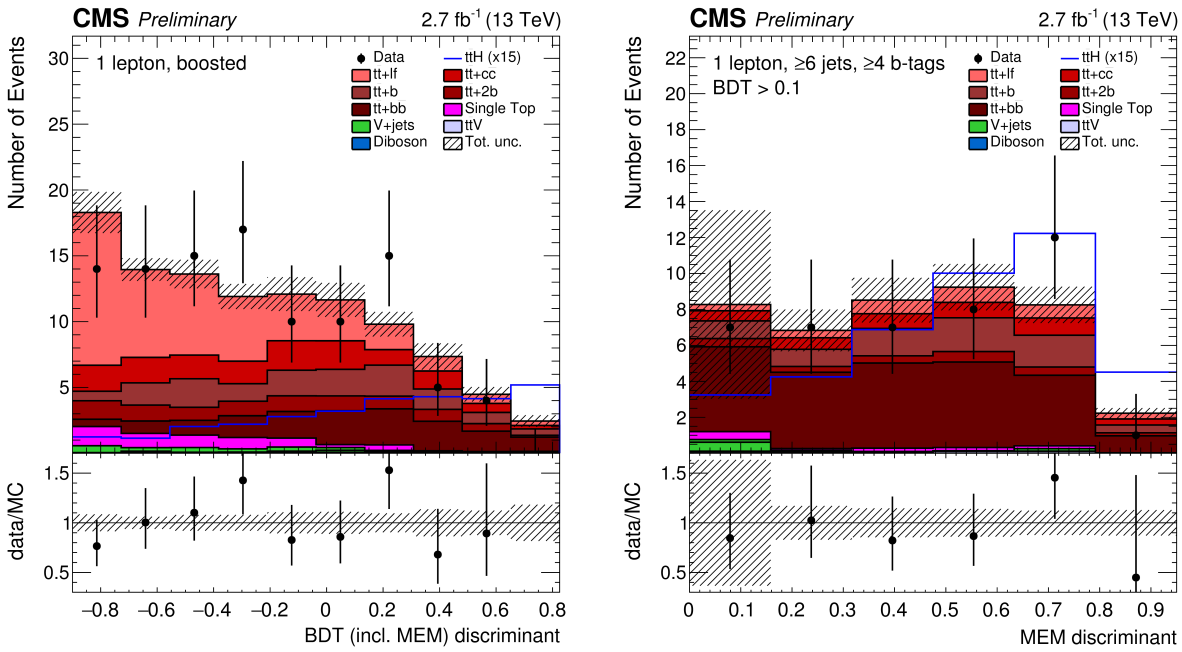

Figure 6 – Final BDT discriminant including the MEM discriminant as input variable for the boosted l+jets category (left), and final MEM discriminant in the signal-like region selected by requiring the BDT discriminant above 0.1 in the l+jets category with at least 6 jets and at least 4 b-tags (right), both are post-fit. The signal is scaled with a constant factor 15 for visibility.

a boosted category is introduced in the l+jets channel for the first time; a fat-jet algorithm is applied to find all decay products of a heavy particle in one jet, then the hadronically decaying top quark and the Higgs boson are identified using substructure information. An l+jets event which matches a multiplicity-based and the boosted category is assigned to the boosted one.

To achieve optimal signal separation a distinct classifier is constructed in each of the 13 categories. In each a BDT with different variables is employed, which is also the final discriminant in the dilepton categories and in the l+jets category with exactly 2 b-tags. An example from the most signal-like dilepton category shows in Figure 5 one of the input variables and the final BDT discriminant. Shown is the dijet mass of the b-tagged jet pair with minimal spatial separation in ΔR, which has a certain probability to be the jet pair from the Higgs boson decay in $\mathrm{t\bar{t}H(b\bar{b})}$, or the additional b jet pair in $\mathrm{t\bar{t}+b\bar{b}}$. It confirms that one can employ m_{H}, the backround shows a non-resonant falling spectrum with a kinematic lower edge from the jet selection while the signal has an enhancement around m_{H}, but that on the other hand the separation is not sufficient to use such a distribution as final discriminant. The other l+jets categories include in addition to the BDT a discriminant from a matrix element method (MEM), which was already developed for Run 1 [8] and further optimized. It gives the probability of a $\mathrm{t\bar{t}H}$-like topology over the background hypothesis, where $\mathrm{t\bar{t}+b\bar{b}}$ is considered. All jet-quark associations are permuted in the calculation, as the association is ambiguous. In categories with exactly 3 b-tags and in the boosted category, the MEM discriminant is used as input variable in the BDT. In categories with at least 4 b-tags, where the MEM deploys its full strength, a two-dimensional analysis of the two discriminators is performed: the events are separated according to their BDT value into more background-like and signal-like events, and in each independently the MEM is considered as final discriminant. Examples are given in Figure 6 for the usage of MEM as input for the final BDT discriminant in the boosted category, and for the two-dimensional approach in the most signal-like l+jets category with at least 6 jets and at least 4 b-tags.

Results are obtained from a simultaneous fit of all categories. The signal strength is in the dilepton channel $\mu = -4.7^{+3.7}_{-3.8}$ below, and in the l+jets channel $\mu = -0.4 \pm 2.1$ around, the SM prediction. The combined result yields $\mu = -2.0 \pm 1.8$, and is 1.7σ below the SM expectation.

The result is dominated by systematic uncertainties, especially the imperfect knowledge of the background, but more data will help to constrain several uncertainties stronger and to better understand the backgrounds together with improvements from theory and modelling.

2.4 $t\bar{t}H$ Combination

A combined $t\bar{t}H$ result [9] is obtained from a fit of the three statistically independent analysis channels described above for $m_H = 125\,\text{GeV}$, correlating common systematic uncertainties. The value of $\mu_{t\bar{t}H} = 0.15^{+0.95}_{-0.81}$ agrees with the SM expectation of $\mu^{SM}_{t\bar{t}H} = 1.00^{+0.96}_{-0.85}$, also in sensitivity.

3 Conclusions and Outlook

First results of $t\bar{t}H$ at $\sqrt{s} = 13\,\text{TeV}$ are presented. Independent analyses are performed according to different Higgs decays in the $t\bar{t}H(\gamma\gamma)$, $t\bar{t}H(\text{multileptons})$ and $t\bar{t}H(b\bar{b})$ channels, each of them using an own analysis strategy. In $t\bar{t}H(\gamma\gamma)$ the signal is extracted from a fit to the invariant diphoton mass distribution and results in a signal strength of $\mu = 3.8^{+4.5}_{-3.6}$. The other two analyses use multi-variate discriminants to achieve good signal-to-background separation. The $t\bar{t}H(\text{multileptons})$ result is $\mu = 0.6^{+1.4}_{-1.1}$, the one of $t\bar{t}H(b\bar{b})$ yields $\mu = -2.0 \pm 1.8$. The $t\bar{t}H(b\bar{b})$ result is 1.7σ below the SM expectation. The other two channels agree within uncertainties with the SM, as well as the combined $t\bar{t}H$ result of $\mu_{t\bar{t}H} = 0.15^{+0.95}_{-0.81}$ considering all three channels.

Sensitivity similar to the Run 1 analysis is achieved by improved analysis techniques, which build the foundation for further analyses; many more results will come with incoming data, already in 2016 the expected integrated luminosity should be roughly a factor 10 more. The observation of $t\bar{t}H$ and the measurement of the top-Higgs Yukawa coupling are amongst the priorities for Run 2. This will allow to confront the SM coupling prediction with data, and is the key to find hidden loop contributions in couplings of the Higgs to gluons or photons. The $t\bar{t}H$ process will be of importance throughout the whole life span of LHC.

References

1. ATLAS Collaboration, Observation of a new particle in the search for the Standard Model Higgs boson with the ATLAS detector at the LHC, *Phys. Lett.* B **716**, 1 (2012).
2. CMS Collaboration, Observation of a new boson at a mass of 125 GeV with the CMS experiment at the LHC, *Phys. Lett.* B **716**, 30 (2012).
3. ATLAS and CMS Collaborations, Measurements of the Higgs boson production and decay rates and constraints on its couplings from a combined ATLAS and CMS analysis of the LHC pp collision data at $\sqrt{s} = 7$ and 8 TeV, ATLAS-CONF-2015-044, CMS-PAS-HIG-15-002.
4. CMS Collaboration, First measurements of the Higgs boson production in the diphoton decay channel at $\sqrt{s} = 13\,\text{TeV}$, CMS-PAS-HIG-15-005.
5. CMS Collaboration, Search for $t\bar{t}H$ production in multilepton final states at $\sqrt{s} = 13\,\text{TeV}$, CMS-PAS-HIG-15-008.
6. CMS Collaboration, Search for $t\bar{t}H$ production in the $H \to b\bar{b}$ decay channel with $\sqrt{s} = 13\,\text{TeV}$ pp collisions at the CMS experiment, CMS-PAS-HIG-16-004.
7. CMS Collaboration, Measurement of $t\bar{t}$ production with additional jet activity, including b quark jets, in the dilepton decay channel using pp collisions at $\sqrt{s} = 8\,\text{TeV}$, arXiv:1510.03072 (accepted by *Eur. Phys. J.* C).
8. CMS Collaboration, Search for a standard model Higgs boson produced in association with a top-quark pair and decaying to bottom quarks using a matrix element method, *Eur. Phys. J.* C **75**, 251 (2015).
9. CMS Collaboration, $t\bar{t}H$ Combination, https://twiki.cern.ch/twiki/bin/view/CMSPublic/TTHCombMoriond2016.